Breast Cancer Research

Contribution of CXCL12 secretion to invasion of breast cancer cells

Breast Cancer Research 2012, **14**:R23 doi:10.1186/bcr3108

Pamela J Boimel (pamela.boimel@med.einstein.yu.edu)
Tatiana Smirnova (tatiana.smirnova@phd.einstein.yu.edu)
Zhen Ni Zhou (zhenni.zhou@med.einstein.yu.edu)
Jeffrey Wyckoff (jeffrey.wyckoff@einstein.yu.edu)
Hae In Park (haein.park@einstein.yu.edu)
Salvatore J Coniglio (salvatore.coniglio@einstein.yu.edu)
Purvi Patel (ppatel@medusa.bioc.aecom.yu.edu)
Bin-Zhi Qian (binzhi.qian@einstein.yu.edu)
E RICHARD Stanley (richard.stanley@einstein.yu.edu)
Anne R Bresnick (anne.bresnick@einstein.yu.edu)
Dianne Cox (dianne.cox@einstein.yu.edu)
Jeffrey W Pollard (jeffrey.pollard@einstein.yu.edu)
William J Muller (william.muller@mcgill.ca)
John Condeelis (john.condeelis@einstein.yu.edu)
Jeffrey E Segall (jeffrey.segall@einstein.yu.edu)

ISSN 1465-5411

Article type Research article

Submission date 29 June 2011

Acceptance date 7 February 2012

Publication date 7 February 2012

Article URL http://breast-cancer-research.com/content/14/1/R23

Contribution of CXCL12 secretion to invasion of breast cancer cells

**Pamela Boimel [1#], Tatiana Smirnova[1#], Zhen Ni Zhou[1], Jeffrey Wyckoff [1,2],Haein Park[1], Salvatore J Coniglio [1], Purvi Patel[3], Bin-Zhi Qian[4], E Richard Stanley[4], Anne R Bresnick [3], Dianne Cox[1,2,4], Jeffrey W Pollard[4,6], William J Muller [5], John Condeelis[1,2], Jeffrey E Segall [1,2]*

[1]Department of Anatomy and Structural Biology, Albert Einstein College of Medicine, Bronx, NY, USA
[2]Gruss Lipper Center for Biophotonics, Albert Einstein College of Medicine, Bronx, NY, USA
[3]Department of Biochemistry, Albert Einstein College of Medicine, Bronx, NY, USA
[4]Department of Developmental and Molecular Biology, Albert Einstein College of Medicine, Bronx, NY, USA
[5]McIntyre Medical Building, 3655 Promenade Sir William Osler, Room 802, Montreal, Quebec H3G 1Y6, Canada
[6] Center for the Study of Reproductive Biology and Women's Health, Albert Einstein College of Medicine, New York, New York 10461, USA

[#]These authors contributed equally to the manuscript.

*Corresponding author: jeffrey.segall@einstein.yu.edu

Abstract

Introduction

Neu (HER2/ErbB2) is over-expressed in 25-30% of human breast cancer, correlating with a poor prognosis. Previous studies using the Neu transgenic mouse model (MMTV-Neu) demonstrated that the Neu-YB line had increased production of CXCL12 and increased metastasis, while the Neu-YD line had decreased metastasis. This study examines the role of increased production of CXCL12 in tumor cell invasion and malignancy.

Methods

We studied invasion in the tumor microenvironment using multiphoton intravital imaging, *in vivo* invasion, and intravasation assays. CXCL12 signaling was altered by using the CXCR4 inhibitor AMD3100 or increasing CXCL12 expression. The role of macrophage signaling *in vivo* was determined using a colony stimulating factor-1 (CSF-1) receptor blocking antibody.

Results

The Neu-YD strain was reduced in invasion, intravasation, and metastasis compared to the Neu-YB and Neu-NDL strains. Remarkably, for the Neu-YB strain, *in vivo* invasion to epidermal growth factor was dependent on both CXCL12/CXCR4 and CSF1/CSF1R signaling. Neu-YB tumors had increased macrophage and microvessel density. Over-expression of CXCL12 in MTLn3 cells increased *in vivo* invasion, as well as microvessel and macrophage densities.

Conclusions

Expression of CXCL12 by tumor cells results in increased macrophage and microvessel density and *in vivo* invasiveness.

Introduction

Neu (HER2/ErbB2) is overexpressed in 25-30% of human breast cancer, correlating with a poor prognosis [1]. Neu is a member of the ErbB family of receptor tyrosine kinases which are important mediators of signal transduction for proliferation, survival, apoptosis, motility, and invasion of cells. The ErbB receptors, consisting of ErbB1 (EGFR), Her2/Neu (ErbB2), ErbB3 and ErbB4, can homodimerize and heterodimerize, mediating ligand specificity and various signal transduction pathways [2]. At low expression levels, Neu is unlikely to homodimerize [3], however it is the preferred binding partner for the other ErbB receptor tyrosine kinases and mediates the activation of potent signal transduction pathways [4, 5].

At high expression levels Neu can homodimerize[6, 7], and the correlation of high levels of expression with poor prognosis and clinical significance as a pharmacological target has made the Neu receptor and its contributions to metastasis and tumorigenesis important areas of study. Due to its clinical significance, the Her2/Neu receptor has been the focus of studies aiming to pharmacologically inhibit its function. Trastuzumab (Herceptin), a human monoclonal antibody, has been used to treat patients with Her2 positive breast cancer [8]. However, the development of drug resistance to trastuzumab treatment [9] underscores the necessity to continue to investigate new ways to pharmacologically inhibit the receptor. To study the Neu receptor *in vivo*, a small deletion, mimicking that found in patient tumors [10], was made in the extracellular domain and this construct (termed Neu-NDL) was expressed by the mammary MMTV promoter in transgenic mice [10, 11]. A series of mutations of Neu-NDL were made in which the major C-terminus phosphorylated tyrosine residues were mutated to

phenylalanine and then individual tyrosines were added back and referred to as YA(1028), YB (1144), YC (1201), YD (1227), and YE (1253) [12].

Using these addback mutants, the contributions of these tyrosine sites to tumorigenesis and lung metastasis were studied in transgenic mice and indicated that the YA site impaired transformation/tumorigenesis, the YB line had increased and the YD decreased metastasis while the other add-back mutants exhibit metastasis rates similar to Neu-NDL [12-14]. Metastasis is a series of steps involving, tumor growth, angiogenesis, motility in the tumor microenvironment, invasion, intravasation, extravasation, and finally growth of metastases at a distant site such as the lungs [15]. We chose to study how the YB and YD sites diverge in their contributions to early stages of metastasis using the Neu transgenic mouse model and *in vivo* assays for tumor cell motility, invasion and intravasation.

It has been shown that the YB line tumors express more CXCL12 (SDF-1) by microarray and ELISA compared to the other lines [14]. CXCL12 binds to the G-protein coupled receptor CXCR4, which is often overexpressed in breast cancer and has been correlated with poor clinical outcome [16, 17]. CXCL12/CXCR4 signaling has been shown to play a role in tumor growth, invasion, angiogenesis, and bone marrow cell recruitment [18-23]. Recent studies of autocrine CXCL12 signaling indicated that it can induce the differentiation of monocytes into a distinct population of pro-angiogenic, immunosuppressive macrophages in the tumor microenvironment [24]. These studies indicate that overexpression of CXCL12 in the tumor microenvironment may alter the invasive capacity, as well as the tumor associated immune cells which are recruited to tumors. CXCL12 overexpression has been linked to increased metastasis and poor

prognosis [25]. Targeting the CXCL12/CXCR4 signaling pathway has also been studied in breast cancer treatment [26, 27]. In this manuscript, we report that increased expression of CXCL12 by breast cancer cells can lead to enhanced *in vivo* invasion and increased macrophage and microvessel density.

Materials and methods

Animal models and cell lines

Procedures involving all mice were conducted in accordance with NIH regulations on the use and care of experimental animals. This mouse study was approved by the Albert Einstein College of Medicine animal use committee. FVB mice transgenic for Neu containing a small activation deletion (Neu-NDL), and the addback mutants Neu-YB and Neu-YD, [10, 11], driven by the MMTV LTR were studied. Mice were followed for tumor growth and were used for experiments when the largest tumor reached 2cm in diameter. Tumor volume was calculated as $l \times w^2/2$. For intravital imaging, the strains, were crossed with a strain expressing the cyan fluorescent protein, CFP, using the mammary gland specific MMTV promoter (MMTV-icre-CAG-CAC-ECFP) as previously described [28, 29]. Xenograft tumors were made by detaching MTLn3 tumor cells with PBS-2mM EDTA and injecting $1x10^6$ cells, resuspended in PBS with 0.35% BSA (w/v), into the right fourth mammary fat pad from the head of 5-7 week old female severe combined immunodeficient (SCID) mice (NCI). Xenograft tumors were grown until they reached 1.5 cm (about 4 weeks) in diameter for the *in vivo* invasion assay.

For culturing, primary tumors were chopped into small pieces, washed in phosphate buffered saline, PBS, and dissociated in PBS with collagenase IV (final

concentration of 6 mg/ml, C5138, Sigma), hyaluronidase (final concentration of 1 mg/ml, H3506, Sigma), and DNase I (final concentration of 0.25 mg/ml, D5025-15KU, Sigma) for 30 minutes with continuous agitation at 37 degrees Celsius. Following digestion, samples were washed twice in sterile PBS and plated in DMEM/F12 (MT10092CV, Fisher Scientific) supplemented with 10% Fetal bovine serum (100-106; Gemini Bio-Products), FBS, and 0.5% penicillin/streptomycin (15140-122, Invitrogen), 1ug/mL hydrocortisone (h4001, Sigma), 10ug/mL Insulin (I5523, Sigma), 1nM cholera toxin (C8052, Sigma), Non-essential amino acids, 10nM EGF (Life Technologies).

To overexpress mouse CXCL12, a pCMVSport6-CXCL12 plasmid (accession number BC006640, EMM1002-4021797, Open Biosystems) was blunt-subcloned into the NOT I restriction site of the pQCXIP vector and confirmed by plasmid sequencing. Retrovirus was generated by transfection of 293-GP cells using lipofectamine 2000 (11668-019, Invitrogen) with 12 μg of plasmid DNA and 4μg of VSV-g plasmid. After 48 hours, supernatants were collected and used to transduce MTLn3-GFP mammary adenocarcinoma cells [30] in the presence of 4μg/mL polybrene. All MTLn3 cell lines were grown in alpha MEM media supplemented with 5%FBS and 0.5% penicillin/streptomycin. Transduced cells were selected with 1μg/ml puromycin. To confirm expression of CXCL12, MTLn3 cells were seeded in 6 well dishes in triplicate and supernatants were collected 16 hours after cultures were confluent. Cells were counted at the time of collection for quantifying the amount in pg/mL for 10^6 cells. For evaluating CXCL12 secreted in vitro by the Neu primary tumor cell lines, dissociated tumor cells were seeded at equal density in 6 well dishes and supernatants were collected 16 hours after cells were confluent. Samples were spun down to remove debris, frozen on

dry ice and stored at -80 degrees Celsius. CXCL12 was measured in the supernatant by ELISA (DY460, R&D systems)., with triplicate measurements done per sample and the amount of CXCL12 in pg/mL was calculated using a standard curve from serial diluted CXCL12 provided in the ELISA kit. MTLn3-GFP cells transduced with JP1520 vector expressing CXCR4 were kindly provided by Dr. Lorena Hernandez [31].

Immunohistochemistry

Tumors were fixed in 10% buffered formalin for a minimum of 24 hours, paraffin embedded and sectioned for H&E. Tumors were also fixed in **p**eriodate-**l**ysine-2% **p**araformaldehyde- 0.05% **g**lutaraldehyde [32] (PLPG), at 4 degrees Celsius overnight and then stored in 70 % ethanol at 4 degrees Celsius until paraffin embedded. PLPG fixed tumors were stained with F4/80 antibody at 1:50 to identify macrophages as previously described [33]. To quantify F4/80 staining, we chose 10 random fields of healthy tumor parenchyma, and counted the number of F4/80 stained macrophages using a 40x objective for N = 3 tumors per strain. We found that formalin fixed tumor vessels were poorly stained by anti-CD34 antibodies, and therefore, to stain tumor vasculature, formalin fixed, paraffin embedded tumor sections were stained with a Rat monoclonal anti-mouse endomucin (V.7C7) antibody (sc-65495, Santa Cruz biotechnology) at 1:50.To quantify endomucin staining, 10 random fields of healthy tumor parenchyma were counted for endomucin stained vessels using a 20x objective for N = 3 tumors per strain. To detect tumor lymphatic vessels, formalin fixed, paraffin embedded tumor sections were stained with a rabbit polyclonal anti-mouse LYVE-1antibody (ab14917, Abcam) at 1:200. Anti-CXCR4 antibody was used at 1:300 (ab7199, Abcam).

To quantify lung metastasis in the Neu transgenic tumors, lung samples were fixed in 10% neutral formalin buffer, embedded in paraffin, sectioned at 5 μm and stained by H&E. H&E sections spaced 250 um apart were taken through the whole lung sample and all micrometastases were counted in every section using a 10x objective on a light microscope. The efficiency of lung metastasis was expressed in total number of metastases in all lung sections for each animal with metastases. To quantify lung metastasis in the MTLn3 pQCXIP and pQCXIP-CXCL12 tumors, lungs were removed after 4 weeks when tumors reached 1.5 cm in size and fixed in 10% neutral formalin buffer, embedded in paraffin, sectioned, and stained by H&E to quantify the total number of lung metastases in all lobes per section with a 10x objective on a light microscope.

In vivo invasion assay

Tumors were allowed to reach 2 cm (Neu transgenic strains) or 1.5 cm (MTLn3 xenografts) in diameter for use in the *in vivo* invasion assay. The collection of the invasive cell population from the primary tumor into microneedles containing matrix and chemoattractant using an *in vivo* invasion assay has been previously described [34]. Mice were anesthetized with Aerrane (isoflurane, Baxter Pharmaceutical Products, Inc., Deerfield, IL) over the course of the assay. Briefly, tumors were first penetrated with 33-gauge Hamilton needles (14-815-423, Fisher) and then these needles were replaced with ones filled with L15, 0.35% BSA containing 10% matrigel (356234, Beckton Dickinson) with or without chemoattractant. Invasive cells were collected for 4 hours and then the contents of the needles were extruded using 0.5 μg/ml DAPI in PBS onto a coverslip for quantifying the number of invasive cells using an Olympus IX70 inverted microscope with a 10× NA 0.30 objective. The chemoattractant EGF (53003018, Gibco Life

Technologies) was used at a concentration of 25nM. To inhibit the CXCR4 receptor, the inhibitor AMD3100 (A5602, Sigma) was used at 0.5μM. To block/neutralize the CSF-1 receptor a purified, monoclonal anti-mouse CSF-1R antibody AFS98 [35], kindly provided by Dr. Richard Stanley, was used at 15 μg/mL. As a control antibody, a mouse IgG antibody was used at the same concentration used for the experimental CSF-1R antibody (012-000-007, Jackson ImmunoResearch).

In vitro invasion assay of MTLn3 cell lines

To evaluate *in vitro* invasion, MTLn3 cells were allowed to invade into a layer of collagen with or without macrophages as previously described [36]. MTLn3 cells were plated on MatTek dishes with or without BAC1.2F5 cells and overlaid with 6 mg/ml collagen I. Cells were allowed to invade over 24 hours and fixed for analysis. To quantify invasion, GFP fluorescence was measured in z sections, taken on a confocal microscope every 5 μm. Sections 20 μm and above were summed and divided by the total GFP fluorescence in all sections. Data are means of 3 separate experiments, each done in triplicate.

Wound healing assay

Primary tumor cells were cultured for one week, passaged into a new 10cm culture dish, and allowed to grow to confluence. EGF was removed from the media 24 hours prior to wound healing assays. Cultures for each of the strains were starved in DMEM/F12, 0.7 % BSA (w/v) for 4 hours and then a grid was drawn on the plate for reference and 4 scratches introduced using a pipette tip. Images were taken at time 0 and cultures were treated with buffer, and 5nM EGF. The Neu-YB strain was also treated with 5nM EGF + 100nM AMD3100, 5nM EGF + 1nM CXCL12, and 1nM CXCL12.

The wound was allowed to heal for 12 hours and images were taken of the same field. Analysis was done using Tscratch software, previously described [37], and the percentage of the wound area closed was calculated.

Chemotaxis assays

Murine bone marrow-derived macrophages (BMMs) were isolated as described previously [38], and were grown in α–MEM containing 15% FBS, 360 ng/ml recombinant human CSF-1 (Chiron, Emeryville, CA) and antibiotics. Cell migration was measured using a transmigration chamber assay with 8 μm pore size inserts (Falcon), according to the manufacturer's instructions. Briefly, the inserts were placed into 24-well plates containing α–MEM in the presence or absence of 50 ng/ml CXCL12. Cells (n=1x10^6) were then loaded onto the inserts and incubated at 37°C for 4 hours. Cells that had migrated through the inserts were counted using phase microscopy and the average number of cells in 5 different fields was calculated. For MTLn3-GFP-CXCR4 cells, a 48-well microchemotaxis chamber (Neuroprobe, Cabin John, MD) was used as described previously [39]. Briefly, cells were starved for 3 hours in L15 media supplemented with 0.35% BSA (L15B) at 37 °C. Two hours prior to microchemotaxis chamber assembly, an 8 μm pore filter (Neuroprobe) was coated with 3.53 mg/ml rat tail collagen type I (BD Biosciences, #354249) in Ca^{2+} or Mg^{2+}-free DPBS. After starvation, cells were detached using PBS-EDTA and 30,000 cells per well loaded into the top wells of the chamber in L15B. Cells were allowed to migrate for 4 hours at 37 °C with bottom wells filled with CXCL12 diluted in L15B, or L15B alone. The filter was then taken out, fixed in 10% paraformaldehyde for 1 hour, nonmigrating cells were removed from the top surface of the filter, and the remaining cells on the lower surface stained overnight with

hematoxylin (Fisher, CS402-1D). The membrane was washed in de-ionized water and migrated cells counted using a light microscope.

Immunofluorencence Microscopy

Live, non-permeabilized murine bone marrow-derived macrophages (BMMs) were stained with anti-CXCR4 antibody (abcam, Cat.No. ab7199) at 1:250 and Alexa Fluor 568 donkey anti-rabbit IgG. Images were taken using the X60 oil/1.40 phase 3 objective of an olympus IX71microscope coupled to CCD camera.

qRT-PCR:

mRNA was isolated from cells in culture, and 100 ng cDNA was used for qRT-PCR. Specific primers for mouse CXCR4 (Fwd: 5'-TGGTGTTTCAATTCCAGCAT-3' and rev: 5'-CGATGCTCTCGAAGTCACAT-3') were from RealTimePrimer.com (Cat.No. VMPS-1496) were used with SYBR green master mix (Superarray PA-012).

Blood burden assay

Mice were anesthetized with Aerrane and blood was taken from the right atrium via cardiac puncture using a 25-gauge needle and 1 mL syringe coated with and containing 0.1 mL heparin. Blood (0.5-1 mL) was drawn and plated into 10 cm dishes filled with DMEM/F12, 20% FBS. The next day, the plates were replaced with fresh medium. After 7 days the number of individual cells in the dish was counted. Tumor blood burden (tumor cells/ mL of blood) was calculated as total number of tumor cells in the dish divided by the volume of blood taken.

Intravital imaging

Animals with an average tumor diameter of 2cm were placed under isoflurane anesthesia and a skin flap surgery was performed to expose the tumor. The animal was

placed on an inverted microscope with continuous anesthesia and tumor cells were imaged using a Radiance 2000 MP multiphoton or on an Olympus Fluoview FV1000-MPE microscope. The CFP fluorescence was at a wavelength of 880nm using a 20X 0.75 NA water objective with a 3x zoom or a 25X 1.05NA water objective with a 2.3x zoom. Time lapse imaging was done over 30 minutes, taking 2 minute intervals, collecting a 100μm stack. Motility was assessed using ImageJ and the average total cell motility was quantified per 50 um z-stack (5 sections imaged at 10 um intervals). A motile cell was defined as any protrusion at least ½ a cell diameter in length.

Results

1.1. The Neu-YD strain exhibits decreased spontaneous invasion, intravasation and metastasis compared to the Neu-NDL and Neu-YB strains.

Metastastic properties were compared between animals with similar tumor volumes. At the time of analysis, the total tumor volume averaged 3-3.5 cm^3 and the largest tumor averaged 2-2.5 cm^3 (Figures 1A and 1B). Interestingly, the Neu-YD strain grew tumors the fastest, taking an average of 24 weeks compared to about 30 weeks for the Neu-NDL and Neu-YB strains (Figure 1C). Despite growing tumors faster ($p < 0.005$), the Neu-YD strain had decreased invasion, intravasation and metastasis (Figure 2). We evaluated invasion using the *in vivo* invasion assay previously described [34], inserting micro needles into the tumor containing EGF and Matrigel to collect the invasive cell population. The Neu-YD tumor cells were significantly less invasive to EGF compared to the Neu-YB and the Neu-NDL strains (Figure 2A). To determine if the decreased invasion of the YD strain correlated with a decreased number of tumor cells in the blood, we evaluated intravasation. The number of intravasated cells for the Neu-YD strain was approximately 200 per mL of blood. This was significantly decreased compared to the Neu-YB which averaged 850 cells per mL or the Neu-NDL strain averaging 940 cells per mL (Figure 2B). The numbers of spontaneous metastases were counted in H&E sections through all lobes of the lungs in mice containing metastases. The Neu-YD strain had significantly fewer metastases than the Neu-YB or Neu-NDL strains (Figure 2C). This indicates the YB site, but not the YD, is sufficient for lung metastasis. These results suggest that the defect in Neu-YD metastasis is due to defects in invasion and intravasation. To determine if defects in invasion and intravasation

correlated with motility in the tumor microenvironment, we used intravital multiphoton microscopy to evaluate tumor cell motility *in vivo* (Figure 3, Additional Files 1- 3). We found that the Neu-YD tumors had slightly fewer motile cells than Neu-NDL. Neu-YB tumors had significantly more motile cells than either the Neu-NDL or Neu-YD tumors.

1.2 The Neu-YB strain has more macrophages in the tumor parenchyma than the Neu-YD and the Neu-NDL strains.

In addition to our findings that the Neu-YB strain had increased invasion, intravasation, metastasis, and motility compared to the Neu-YD strain, it has also been shown to be unique in its tumor morphology and expression profile compared to the other Neu lines [14, 40]. Our past studies have focused on the role of macrophages in a tumor cell and macrophage paracrine loop driving *in vivo* invasion [36, 41]. We were interested to see if differences in the number of macrophages in the tumor correlated with the differences we found in Neu-YB and Neu-YD *in vivo* invasion and tumor cell motility. We found that the Neu-YB tumors had on average twice the number of F4/80 positive macrophages compared to the Neu-YD tumors (per mm^2, $p < 0.0005$, and also had significantly more than the Neu-NDL control, $p < 0.05$) (Figures 4A and 4B). The Neu-YD strain also had fewer macrophages than the Neu-NDL, $p < 0.005$. In addition to macrophage recruitment we looked at the distribution of vasculature and lymphatics in the various strains. We observed no difference in lymphatics (Additional File 4), but saw significantly more vasculature staining in the Neu-YB strain compared to the Neu-NDL ($p < 0.05$) and Neu-YD strains ($p < 0.0005$) (Additional File 5). The Neu-YD strain also had significantly fewer vessels than the Neu-NDL ($p < 0.005$). The increase in

vasculature seen in the Neu-YB strain is consistent with studies in which CXCL12 has been correlated with increased angiogenesis and hematopoesis [23].

1.3 EGF induced *in vivo* invasion of Neu-YB tumor cells is dependent on CXCR4/CXC12 signaling in the tumor microenvironment.

Since the Neu-YB tumor cells have been shown to express more CXCL12 than the other mutants and Neu-NDL [14], we investigated whether CXCR4 signaling played a role in EGF induced *in vivo* invasion in that tumor. EGF induced *in vivo* invasion of the Neu-YB strain was significantly inhibited by the CXCR4 inhibitor AMD3100, $p < 0.0005$ (Figure 5A). The Neu-YD and Neu-NDL tumor cells were not significantly affected by AMD3100 inhibition of CXCR4. This suggested that the CXCL12 expressed by the Neu-YB tumor cells was necessary for EGF induced *in vivo* invasion. We have previously shown that EGF induced *in vivo* invasion in the Neu-NDL model is dependent on a CSF-1/EGF paracrine loop [41]. To test this in the Neu-YB line we used a CSF-1 receptor blocking antibody. The antibody inhibited EGF-induced *in vivo* invasion in the YB strain, as well as the YD and Neu-NDL tumors, confirming that the paracrine loop was still operating (Figure 5B).

To evaluate *in vitro* migration, monolayers were grown from primary cells derived from the Neu-NDL, Neu-YD, and Neu-YB primary tumors *in vitro*, and wound healing assays were done in the presence of EGF, EGF and AMD3100 and CXCL12. There was decreased EGF induced *in vitro* migration in the Neu-YB and Neu-YD strains compared to the Neu-NDL in the wound healing assay, $p < 0.0005$ (Figure 5C). We evaluated CXCL12 secretion by ELISA in the primary cultures and found the Neu-YB

expressed more CXCL12 than the Neu-NDL and the Neu-YD (Additional File 6A). We confirmed in all three tumor types that there are similar levels of CXCR4 receptor (Additional File 6B and C). However, there was no effect of CXCR4 inhibition or stimulation on *in vitro* wound healing in the Neu-YB strain (Figure 5D). The tumor cells did not respond to CXCL12 in a chemotaxis assay either (Additional File 6D). Chemotaxis and wound healing assays with CXCL12 were also performed with MTLn3-CXCR4 overexpressing cells as positive controls (Additional File 6D and E). These studies indicate that the tumor cells are note activated through autocrine stimulation by CXCL12 but rather that a paracrine loop involving CXCR4/CXCL12 signaling in the tumor microenvironment is needed for EGF induced *in vivo* invasion in the Neu-YB tumors.

1.4 Overexpression of CXCL12 in MTLn3 rat adenocarcinoma cells increases *in vitro* and *in vivo* invasion and increases macrophage density in the tumor.

To confirm that CXCL12 secretion by tumor cells can result in an increase in macrophage density and tumor cell in vivo invasion, we overexpressed CXCL12 in MTLn3 cells (Additional File 7). In a 3D *in vitro* macrophage co-invasion assay, MTLn3 cells overexpressing CXCL12 were significantly more invasive through collagen than the empty vector control (Figure 6A). CXCL12 overexpression also significantly increased *in vivo* invasion to EGF compared to the empty vector control (Figure 6B). Similar to the Neu-YB tumors, CXCL12 overexpression in MTLn3 cells increased the number of macrophages present in the tumor parenchyma approximately 2-fold, $p < 0.005$ (Figures 6C and 6D). In addition, we evaluated CXCR4 expression levels on macrophages and

tumor cells in the MTLn3 tumors and found the macrophages in these tumors expressed more CXCR4 than the tumor cells (Additional File 8A). Of note, there was no significant difference in the amount of CXCR4 receptor on macrophages from the CXCL12 overexpressing tumors compared to the control, (Additional File 8A). Moreover, we demonstrated that CXCL12 induced the migration of CXCR4-positive macrophages (Additional File 8B and C). CXCL12 overexpression had no effect on tumor size. However, we did observe a trend of increased numbers of metastases with CXCL12 expression (Additional File 9A and B). Consistent with our observation that the Neu-YB tumors, which express increased amounts of CXCL12, have a higher microvessel density, we confirmed that CXCL12 expression in MTLn3 cells also significantly increases the number of blood vessels in the primary tumors as compared to control MTLn3 tumors (Additional File 9C-E).

Discussion

In this paper, we find that expression of CXCL12 by breast tumor cells can enhance in vivo invasion in the tumor microenvironment through recruitment of macrophages. We initially analyzed the Neu transgenic tumors. The Neu-YB and Neu-YD strains had different metastatic capacities, consistent with previously published data [14]. We found that the Neu-YD tumor cells are defective in wound healing *in vitro* and this correlates with decreased *in vivo* invasion in the primary tumor and decreased metastasis to the lungs. The Neu-YB tumor cells showed a reduction in wound healing *in vitro* similar to that of the Neu-YD cells. However, in vivo they exhibited increased motility compared to both the Neu-NDL and Neu-YD strains and increased in vivo invasion, intravasation and metastasis compared to the Neu-YD strain. The increased *in vivo* invasion was dependent on CXCR4 function, consistent with the overexpression of CXCL12 by Neu-YB tumors. We then directly tested the role of CXCL12 expression in tumor cells by overexpressing this ligand in MTLn3 cells. Increased CXCL12 expression in MTLn3 cells resulted in increased *in vivo* invasion, macrophage density, and microvessel numbers, consistent with our observations in Neu-YB tumors.

The CXCR4/CXCL12 signaling axis contributes to metastasis and clinical outcome in breast cancer. CXCR4 expression in breast cancer cells has been shown to increase metastasis by homing of tumor cells to sites of increased CXCL12 expression such as the lymph nodes [16]. Overexpression of CXCL12 increased in vitro invasion and migration of human breast cancer MDA-MB 231 cells [25] , and overexpression of CXCL12 was seen in breast cancer patients with lymph node positive, metastatic disease with a poor prognosis [25]. We have directly evaluated the role of increased CXCL12

expression in *in vivo* tumor cell invasion, where the tumor microenvironment and paracrine loops with supporting stromal cells can influence tumor cell behavior. We find that inhibiting CXCR4 with AMD3100 reduced Neu-YB *in vivo* invasion to EGF to levels similar to Neu-YD. This indicates that invasion to EGF is dependent on CXCL12/CXCR4 signaling in the tumor microenvironment specifically in the Neu-YB strain.

We also saw increased numbers of macrophages in the Neu-YB tumor parenchyma. Since there is an EGF/CSF1R paracrine loop with macrophages inducing tumor cell invasion, we tested whether CXCL12 was acting on the Neu-YB tumor cells to increase invasion in an autocrine manner or in a paracrine loop with macrophages. As we have shown previously for the EGF-CSF1 paracrine loop [36], a blocking antibody to the CSF-1 receptor decreased *in vivo* invasion in the YB strain, indicating that *in vivo* invasion of the YB tumor cells was still dependent upon the EGFR/CSF1R paracrine loop interaction with macrophages. *In vitro*, we found that both Neu-YB and Neu-YD primary tumor cells had impaired wound healing to EGF compared to the Neu-NDL cells. Addition of CXCL12 did not increase *in vitro* wound healing in the Neu-YB cultures, and AMD3100 did not inhibit it, supporting the hypothesis that in this model CXCL12 contributes to a paracrine loop between tumor cells and macrophages within the tumor microenvironment. We hypothesize that the increased macrophage recruitment in the Neu-YB tumors results in enhanced paracrine loop invasion which compensates for the reduced inherent invasiveness in the Neu-YB cells. Thus the inherent defect in Neu-YB tumor cell invasiveness is compensated for by increased CXCL12 expression. To confirm that CXCL12 expression can produce such effects, we overexpressed CXCL12 in MTLn3

breast cancer cells and observed increased *in vitro* and *in vivo* invasion as well as increased tumor associated macrophage recruitment.

There are a number of possible mechanisms by which increased CXCL12 expression could enhance tumor invasiveness and malignancy. This study indicates that CXCL12 overexpression itself in different tumor models can recruit more macrophages. The increased recruitment of tumor associated macrophages may induce increased tumor cell motility and invasion simply through increasing the number of macrophages contributing to paracrine loop signaling [36, 42-45]. In addition, secreted CXCL12 signaling to CXCR4 receptors on macrophages can increase EGF receptor ligand shedding [46], and this could also contribute to increased tumor cell motility and invasion. Alternatively, for tumors expressing CXCR4, autocrine signaling has been shown to increase migration and invasion in other models [25, 47]; CXCL12 can transactivate the EGFR and Neu through Src activation [43, 48] and EGF can potentiate CXCL12-driven chemotaxis [49]. Our *in vitro* studies showing that Neu-YB cells are similar to Neu-YD cells in the wound healing *in vitro* assay, with addition of CXCL12 or inhibition of CXCR4 having no effect, argue against autocrine signaling contributing to the invasion of Neu-YB tumor cells.

We also find increased microvessel density in tumors overexpressing CXCL12. Since the tumor cells we have studied in this paper do not show strong responsiveness to CXCL12, this most likely reflects a stromal response to CXCL12. In particular, the increased macrophage density may also give rise to increased angiogenesis through secretion of angiogenic factors such as VEGF [50-53]. Intriguingly, we did not find that this enhanced tumor growth. However, the increased microvessel density could result in

increased intravasation through the presence of a higher density of entrance sites into the blood, with a corresponding increase in formation of metastases.

Conclusion

In summary, we have found that secretion of CXCL12 by breast cancer cells can enhance invasion *in vivo* and recruitment of macrophages to the primary tumor. This enhancement of invasion depends upon CXCR4 signaling, and is most likely through activation of CXCR4 on macrophages resulting in increased paracrine interactions with tumor cells in the tumor microenvironment. Increased CXCL12 secretion also gives rise to increased microvessel density, which may also be mediated by tumor associated macrophages and contributes to an altered tumor architecture. These results demonstrate how tumor cell regulation of the local cellular microenvironment can increase invasion and motility to contribute to enhanced tumor malignancy.

Abbreviations

CSF-1 = colony stimulating factor-1; EGF = epidermal growth factor; Neu-NDL = Neu deletion mutant (activated receptor); MMTV = mouse mammary tumor virus; ELISA = Enzyme-linked immunosorbent assay; SCID: Severe Combined Immune Deficient; FBS = Fetal bovine serum; SDF-1 = stromal cell-derived factor-1; PLPG = **p**eriodate-**l**ysine-2% **p**araformaldehyde- 0.05% **g**lutaraldehyde; LYVE-1 = lymphatic vessel endothelial hyaluronan receptor; MTLn3 = rat mammary adenocarcinoma cell line; BMM = bone marrow-derived macrophages; GFP = green fluorescent protein; CFP = Cyan fluorescent protein; VEGF = vascular endothelial growth factor; SEM = standard errors of the mean

Competing interests

The authors declare that they have no competing interests.

Authors Contributions

PB and TS contributed equally carrying out in vivo and in vitro experiments, data analysis, multiphoton imaging and analysis, and the preparation of this manuscript. PB bred transgenic mice and performed in vivo studies in SCID mice. ZZ carried out additional immunohistochemistry studies for tumor vasculature, as well as additional in vitro wound healing assays and MTLn3 wound healing and chemotaxis assays. JW helped carry out multiphoton imaging and contributed intellectually to the development of this study. JC contributed intellectually to the development of this study and kindly provided reagents. HP and DC carried out in vitro BMM chemotaxis studies and BMM immunoflourescence. SC performed and analyzed qRT-PCR. PP and ARB carried out

and analyzed in vitro invasion assays on MTLn3 cells. JWP provided assistance in breeding transgenic mice and FACS analysis. WJM provided the Neu-NDL, Neu-YB, and Neu-YD mice. BZQ performed FACS analysis during the development of the study and contributed intellectually. ERS provided the PLPG fixation protocol and reagents. JES contributed intellectually in the development and implementation of the study as well as assisting in preparing the manuscript. All authors have read and approved the manuscript for publication.

Acknowledgements

We would like to thank the Condeelis, Cox, Hodgson, and Segall labs for comments and suggestions. J.E.S. is the Betty and Sheldon Feinberg Senior Faculty Scholar in Cancer Research. Funding was provided by GM071828 (HP), CA100324 (ERS, ARB, DC, JWP, JC and JES) and Albert Einstein College of Medicine Cancer Center Grant 5P30-CA13330.

References

1. Slamon DJ, Godolphin W, Jones LA, Holt JA, Wong SG, Keith DE, Levin WJ, Stuart SG, Udove J, Ullrich A, Press MF: **Studies of the HER-2/neu proto-oncogene in human breast and ovarian cancer**. *Science* 1989, **244**(4905):707-712.
2. Yarden Y: **The EGFR family and its ligands in human cancer. signalling mechanisms and therapeutic opportunities**. *Eur J Cancer* 2001, **37 Suppl 4**:S3-8.
3. Klapper LN, Glathe S, Vaisman N, Hynes NE, Andrews GC, Sela M, Yarden Y: **The ErbB-2/HER2 oncoprotein of human carcinomas may function solely as a shared coreceptor for multiple stroma-derived growth factors**. *Proceedings of the National Academy of Sciences of the United States of America* 1999, **96**(9):4995-5000.
4. Tzahar E, Waterman H, Chen X, Levkowitz G, Karunagaran D, Lavi S, Ratzkin BJ, Yarden Y: **A hierarchical network of interreceptor interactions determines signal transduction by Neu differentiation factor/neuregulin and epidermal growth factor**. *Molecular and cellular biology* 1996, **16**(10):5276-5287.
5. Pinkas-Kramarski R, Soussan L, Waterman H, Levkowitz G, Alroy I, Klapper L, Lavi S, Seger R, Ratzkin BJ, Sela M, Yarden Y: **Diversification of Neu differentiation factor and epidermal growth factor signaling by combinatorial receptor interactions**. *Embo J* 1996, **15**(10):2452-2467.
6. Ghosh R, Narasanna A, Wang SE, Liu S, Chakrabarty A, Balko JM, Gonzalez-Angulo AM, Mills GB, Penuel E, Winslow J, Sperinde J, Dua R, Pidaparthi S, Mukherjee A, Leitzel K, Kostler WJ, Lipton A, Bates M, Arteaga CL: **Trastuzumab has preferential activity against breast cancers driven by HER2 homodimers**. *Cancer research* 2011, **71**(5):1871-1882.
7. Landgraf R: **HER2 therapy. HER2 (ERBB2): functional diversity from structurally conserved building blocks**. *Breast Cancer Res* 2007, **9**(1):202.
8. Hudis CA: **Trastuzumab--mechanism of action and use in clinical practice**. *N Engl J Med* 2007, **357**(1):39-51.
9. Nahta R, Esteva FJ: **HER2 therapy: molecular mechanisms of trastuzumab resistance**. *Breast Cancer Res* 2006, **8**(6):215.
10. Siegel PM, Ryan ED, Cardiff RD, Muller WJ: **Elevated expression of activated forms of Neu/ErbB-2 and ErbB-3 are involved in the induction of mammary tumors in transgenic mice: implications for human breast cancer**. *Embo J* 1999, **18**(8):2149-2164.
11. Siegel PM, Dankort DL, Hardy WR, Muller WJ: **Novel activating mutations in the neu proto-oncogene involved in induction of mammary tumors**. *Molecular and cellular biology* 1994, **14**(11):7068-7077.
12. Dankort DL, Wang Z, Blackmore V, Moran MF, Muller WJ: **Distinct tyrosine autophosphorylation sites negatively and positively modulate neu-mediated transformation**. *Molecular and cellular biology* 1997, **17**(9):5410-5425.

13. Dankort DL, Muller WJ: **Signal transduction in mammary tumorigenesis: a transgenic perspective**. *Oncogene* 2000, **19**(8):1038-1044.
14. Schade B, Lam SH, Cernea D, Sanguin-Gendreau V, Cardiff RD, Jung BL, Hallett M, Muller WJ: **Distinct ErbB-2 coupled signaling pathways promote mammary tumors with unique pathologic and transcriptional profiles**. *Cancer research* 2007, **67**(16):7579-7588.
15. Chambers AF, Groom AC, MacDonald IC: **Dissemination and growth of cancer cells in metastatic sites**. *Nature reviews Cancer* 2002, **2**(8):563-572.
16. Muller A, Homey B, Soto H, Ge N, Catron D, Buchanan ME, McClanahan T, Murphy E, Yuan W, Wagner SN, Barrera JL, Mohar A, Verastegui E, Zlotnik A: **Involvement of chemokine receptors in breast cancer metastasis**. *Nature* 2001, **410**(6824):50-56.
17. Salvucci O, Bouchard A, Baccarelli A, Deschenes J, Sauter G, Simon R, Bianchi R, Basik M: **The role of CXCR4 receptor expression in breast cancer: a large tissue microarray study**. *Breast cancer research and treatment* 2006, **97**(3):275-283.
18. Orimo A, Gupta PB, Sgroi DC, Arenzana-Seisdedos F, Delaunay T, Naeem R, Carey VJ, Richardson AL, Weinberg RA: **Stromal fibroblasts present in invasive human breast carcinomas promote tumor growth and angiogenesis through elevated SDF-1/CXCL12 secretion**. *Cell* 2005, **121**(3):335-348.
19. Fernandis AZ, Prasad A, Band H, Klosel R, Ganju RK: **Regulation of CXCR4-mediated chemotaxis and chemoinvasion of breast cancer cells**. *Oncogene* 2004, **23**(1):157-167.
20. Lee BC, Lee TH, Avraham S, Avraham HK: **Involvement of the chemokine receptor CXCR4 and its ligand stromal cell-derived factor 1alpha in breast cancer cell migration through human brain microvascular endothelial cells**. *Mol Cancer Res* 2004, **2**(6):327-338.
21. Kishimoto H, Wang Z, Bhat-Nakshatri P, Chang D, Clarke R, Nakshatri H: **The p160 family coactivators regulate breast cancer cell proliferation and invasion through autocrine/paracrine activity of SDF-1alpha/CXCL12**. *Carcinogenesis* 2005, **26**(10):1706-1715.
22. Petit I, Jin D, Rafii S: **The SDF-1-CXCR4 signaling pathway: a molecular hub modulating neo-angiogenesis**. *Trends Immunol* 2007, **28**(7):299-307.
23. Kryczek I, Wei S, Keller E, Liu R, Zou W: **Stroma-derived factor (SDF-1/CXCL12) and human tumor pathogenesis**. *Am J Physiol Cell Physiol* 2007, **292**(3):C987-995.
24. Sanchez-Martin L, Estecha A, Samaniego R, Sanchez-Ramon S, Vega MA, Sanchez-Mateos P: **The chemokine CXCL12 regulates monocyte-macrophage differentiation and RUNX3 expression**. *Blood* 2011, **117**(1):88-97.
25. Kang H, Watkins G, Parr C, Douglas-Jones A, Mansel RE, Jiang WG: **Stromal cell derived factor-1: its influence on invasiveness and migration of breast cancer cells in vitro, and its association with prognosis and survival in human breast cancer**. *Breast Cancer Res* 2005, **7**(4):R402-410.
26. Epstein RJ: **The CXCL12-CXCR4 chemotactic pathway as a target of adjuvant breast cancer therapies**. *Nature reviews Cancer* 2004, **4**(11):901-909.

27. Duda DG, Kozin SV, Kirkpatrick ND, Xu L, Fukumura D, Jain RK: **CXCL12 (SDF1{alpha})-CXCR4/CXCR7 Pathway Inhibition: An Emerging Sensitizer for Anticancer Therapies?** *Clinical cancer research : an official journal of the American Association for Cancer Research* 2011, **17**(8):2074-2080.
28. Entenberg D WJ, Gligorijevic B, Roussos E, Verkhusha V, Pollard JW, Condeelis J: **Two laser multiphoton microscope and analysis software for multichannel intravital fluorescence imaging**. *Nature Protocols* 2011.
29. Wyckoff J GB, Entenberg D, Segall J, Condeelis J: **High-Resolution Multiphoton Imaging of Tumors In Vivo**. *Cold Spring Harbor* 2011, **Chapter 24**:441-461.
30. Neri A, Welch D, Kawaguchi T, Nicolson GL: **Development and biologic properties of malignant cell sublines and clones of a spontaneously metastasizing rat mammary adenocarcinoma**. *J Natl Cancer Inst* 1982, **68**(3):507-517.
31. Hernandez LM, M. Coniglio, S. Condeelis, J. Segall, J.: **Opposing roles of CXCR4 and CXCR7 in breast cancer metastasis.** *Submitted to Breast Cancer Research* 2011.
32. McLean IW, Nakane PK: **Periodate-lysine-paraformaldehyde fixative. A new fixation for immunoelectron microscopy**. *J Histochem Cytochem* 1974, **22**(12):1077-1083.
33. Gouon-Evans V, Lin EY, Pollard JW: **Requirement of macrophages and eosinophils and their cytokines/chemokines for mammary gland development**. *Breast Cancer Res* 2002, **4**(4):155-164.
34. Hernandez L, Smirnova T, Wyckoff J, Condeelis J, Segall JE: **In vivo assay for tumor cell invasion**. *Methods Mol Biol* 2009, **571**:227-238.
35. Sudo T, Nishikawa S, Ogawa M, Kataoka H, Ohno N, Izawa A, Hayashi S: **Functional hierarchy of c-kit and c-fms in intramarrow production of CFU-M**. *Oncogene* 1995, **11**(12):2469-2476.
36. Goswami S, Sahai E, Wyckoff JB, Cammer M, Cox D, Pixley FJ, Stanley ER, Segall JE, Condeelis JS: **Macrophages promote the invasion of breast carcinoma cells via a colony-stimulating factor-1/epidermal growth factor paracrine loop**. *Cancer research* 2005, **65**(12):5278-5283.
37. Geback T, Schulz MM, Koumoutsakos P, Detmar M: **TScratch: a novel and simple software tool for automated analysis of monolayer wound healing assays**. *Biotechniques* 2009, **46**(4):265-274.
38. Stanley ER: **Murine bone marrow-derived macrophages**. *Methods Mol Biol* 1997, **75**:301-304.
39. Xue C, Liang F, Mahmood R, Vuolo M, Wyckoff J, Qian H, Tsai KL, Kim M, Locker J, Zhang ZY, Segall JE: **ErbB3-dependent motility and intravasation in breast cancer metastasis**. *Cancer Res* 2006, **66**(3):1418-1426.
40. Dankort D, Maslikowski B, Warner N, Kanno N, Kim H, Wang Z, Moran MF, Oshima RG, Cardiff RD, Muller WJ: **Grb2 and Shc adapter proteins play distinct roles in Neu (ErbB-2)-induced mammary tumorigenesis: implications for human breast cancer**. *Molecular and cellular biology* 2001, **21**(5):1540-1551.

41. Hernandez L, Smirnova T, Kedrin D, Wyckoff J, Zhu L, Stanley ER, Cox D, Muller WJ, Pollard JW, Van Rooijen N, Segall JE: **The EGF/CSF-1 paracrine invasion loop can be triggered by heregulin beta1 and CXCL12**. *Cancer research* 2009, **69**(7):3221-3227.
42. Porta C, Subhra Kumar B, Larghi P, Rubino L, Mancino A, Sica A: **Tumor promotion by tumor-associated macrophages**. *Adv Exp Med Biol* 2007, **604**:67-86.
43. Porcile C, Bajetto A, Barbieri F, Barbero S, Bonavia R, Biglieri M, Pirani P, Florio T, Schettini G: **Stromal cell-derived factor-1alpha (SDF-1alpha/CXCL12) stimulates ovarian cancer cell growth through the EGF receptor transactivation**. *Exp Cell Res* 2005, **308**(2):241-253.
44. Hagemann T, Robinson SC, Schulz M, Trumper L, Balkwill FR, Binder C: **Enhanced invasiveness of breast cancer cell lines upon co-cultivation with macrophages is due to TNF-alpha dependent up-regulation of matrix metalloproteases**. *Carcinogenesis* 2004, **25**(8):1543-1549.
45. Wyckoff JB, Wang Y, Lin EY, Li JF, Goswami S, Stanley ER, Segall JE, Pollard JW, Condeelis J: **Direct visualization of macrophage-assisted tumor cell intravasation in mammary tumors**. *Cancer research* 2007, **67**(6):2649-2656.
46. Rigo A, Gottardi M, Zamo A, Mauri P, Bonifacio M, Krampera M, Damiani E, Pizzolo G, Vinante F: **Macrophages may promote cancer growth via a GM-CSF/HB-EGF paracrine loop that is enhanced by CXCL12**. *Mol Cancer* 2010, **9**:273.
47. Rhodes LV, Short SP, Neel NF, Salvo VA, Zhu Y, Elliott S, Wei Y, Yu D, Sun M, Muir SE, Fonseca JP, Bratton MR, Segar C, Tilghman SL, Sobolik-Delmaire T, Horton LW, Zaja-Milatovic S, Collins-Burow BM, Wadsworth S, Beckman BS, Wood CE, Fuqua SA, Nephew KP, Dent P, Worthylake RA, Curiel TJ, Hung MC, Richmond A, Burow ME: **Cytokine receptor CXCR4 mediates estrogen-independent tumorigenesis, metastasis, and resistance to endocrine therapy in human breast cancer**. *Cancer research* 2011, **71**(2):603-613.
48. Cabioglu N, Summy J, Miller C, Parikh NU, Sahin AA, Tuzlali S, Pumiglia K, Gallick GE, Price JE: **CXCL-12/stromal cell-derived factor-1alpha transactivates HER2-neu in breast cancer cells by a novel pathway involving Src kinase activation**. *Cancer research* 2005, **65**(15):6493-6497.
49. Mosadegh B, Saadi W, Wang SJ, Jeon NL: **Epidermal growth factor promotes breast cancer cell chemotaxis in CXCL12 gradients**. *Biotechnol Bioeng* 2008, **100**(6):1205-1213.
50. Qian BZ, Pollard JW: **Macrophage diversity enhances tumor progression and metastasis**. *Cell* 2010, **141**(1):39-51.
51. Lin EY, Li JF, Gnatovskiy L, Deng Y, Zhu L, Grzesik DA, Qian H, Xue XN, Pollard JW: **Macrophages regulate the angiogenic switch in a mouse model of breast cancer**. *Cancer research* 2006, **66**(23):11238-11246.
52. Lazennec G, Richmond A: **Chemokines and chemokine receptors: new insights into cancer-related inflammation**. *Trends Mol Med* 2010, **16**(3):133-144.

53. Lewis JS, Landers RJ, Underwood JC, Harris AL, Lewis CE: **Expression of vascular endothelial growth factor by macrophages is up-regulated in poorly vascularized areas of breast carcinomas**. *J Pathol* 2000, **192**(2):150-158.

Figure legends

Figure 1. Evaluation of tumor growth, burden and age. (A.) Size of largest tumor at time of analysis. There was no significant difference between the Neu-NDL, Neu-YD, or Neu-YB strains. **(B.) Total tumor volume at time of analysis.** Transgenic mice develop multiple tumors. All tumors were measured, and the volumes added. There was no significant difference in cumulative tumor volume, which averaged about $4cm^3$. **(C.) The average age in weeks at time of analysis**. Data are means and SEM, ** $p < 0.005$ by t-test. N = 18-22 mice per strain.

Figure 2. The Neu-YD strain exhibits decreased invasion, intravasation and metastasis compared to Neu-NDL and Neu-YB strains. (A.) The *in vivo* invasion assay was performed, allowing tumor cells to invade over 4 hours into microneedles containing 25nM EGF or buffer. Data are means and standard errors of the mean (SEM), ** $p < 0.005$ by t-test. N = 3-5 mice per strain, 5-7 needles per condition. **(B.)** The blood burden assay was used to evaluate intravasation. The number of single cells/mL of blood were counted. Data are means and SEM, * $p < 0.05$ by t-test. N = 8-11 mice per strain. **(C.)** 5 µm H&E sections spaced 250 um apart were taken through the whole lung sample and metastases were counted in every section. The efficiency of lung metastasis was represented as total number of metastases in all lung sections for each animal which had metastasis. Data are means and SEM, * $p < .05$ and ** $p < 0.005$ by Mann Whitney. N = 16 mice for Neu-NDL, 15 mice for Neu-YD strain, and 8 mice for the Neu-YB strain.

Figure 3. Motility in the tumor microenvironment. Intravital imaging (IVI) using multiphoton microscopy of primary mammary tumors from transgenic Neu-NDL, Neu-YD and Neu-YB cfp mice. Thirty minute time-lapse z-series were collected and the average total cell motility was quantified per 50 um z-stack (5 sections imaged at 10 um intervals). Data are means and standard errors of the mean of 27 – 32 separate z stacks. N = 13 mice for Neu-NDL, N = 8 mice for Neu-YD, N = 12 mice for Neu-YB. *: $p<0.05$, **: $p<0.005$ by Mann-Whitney analysis.

Figure 4. F4/80 staining indicates the Neu-YB strain recruits more macrophages into the tumor parenchyma. **(A.)** Quantification of F4/80 staining was done using a 40x objective, and counting the number of F4/80 stained macrophages per field. N = 3 tumors per strain, 10 random fields/ tumor. Data shown are means and standard errors of the mean, * $p < 0.05$, ** $p < 0.005$, *** $p < 0.0005$ by t-test. **(B.)** Representative fields of F4/80 staining taken at low (***i***.), scale bar = 200μm, and high (***ii.***), scale bar = 25μm, magnifications.

Figure 5. EGF induced *in vivo* invasion is dependent on CXCR4/CXCL12 paracrine signaling in the tumor microenvironment. **(A.)** *In vivo* invasion assay performed using 25nM EGF and EGF + 0.5μM AMD3100 in microneedles placed in the primary tumor to collect the invasive cell population over 4 hours. Data are means and standard errors of the mean (SEM), *** $p < .0005$ by t-test. N = 3-5 mice per strain, 5-7 needles per condition. **(B.)** *In vivo* invasion assay performed with 25nM EGF + control rat IgG antibody, or EGF + CSF1R blocking antibody (αCSF-1R IgG) in the needles.

Data are means and SEM, *** p < .0005 by t-test. N = 3-5 mice per strain, 5-7 needles per condition. **(C.)** *In vitro* wound healing assays in the absence (Buffer) or presence of 5 nM EGF (EGF). Data are means and SEM, * p < 0.05, ** p < 0.005, *** p <0.0005 by t-test. N = 3 tumors per strain, at least 10 fields per condition. **(D.)** *In vitro* wound healing assays were performed with confluent, primary tumor in the presence of buffer (Buffer), 5 nM EGF alone (EGF), 5nM EGF with 100nM AMD3100 (EGF +AMD3100), 5 nM EGF with 1nM CXCL12 (EGF+CXCL12) or 1 nM CXCL12 alone (CXCL12). Data are means and SEM, ** p <0.005 by t-test. N = 3 tumors, at least 10 fields per condition.

Figure 6. MTLn3 CXCL12 cells have increased invasion to EGF and recruitment of macrophages. **(A.)** *In vitro* invasion of MTLn3 cells expressing GFP and either the empty vector control pQCXIP or overexpressing CXCL12 were plated on MatTek dishes with BAC1.2F5 macrophages, overlaid with collagen and allowed to invade. After 24 hours cells invading through the collagen 20 um and above were quantified using a confocal microscope. Data shown are means and standard errors of the mean (SEM), *** p < 0.0005 by t-test. **(B.)** The in vivo invasion assay was done of MTLn3 empty vector and CXCL12 overexpressing cell line tumors, allowing tumor cells to invade over 4 hours in to microneedles containing 25nM EGF or buffer. Data shown are means and SEM, * p < 0.05, *** p < 0.0005 by t-test. **(C.)** Quantification of F4/80 staining was done using a 40x objective, and counting the number of F4/80 stained macrophages per field. N = 5 tumors per cell line, 10 random fields/ tumor. Data shown are means and SEM, ** p < 0.005 by t-test. **(D.)** Representative images of F4/80 staining for macrophages in

MTLn3 pQCXIP and MTLn3 pQCXIP-CXCL12 tumors. Images taken using a 40x objective, scale bar = 25μm.

Additional file legends

Additional Files 1,2 and 3. Supplemental Movies 1, 2, and 3. The Neu-YB (Additional File 3) strain tumors have more motility in the tumor microenvironment than the Neu-NDL (Additional File 1) or Neu-YD (Additional File 2) strains. Tumors were exposed with a skin flap surgery and mice were imaged with a multiphoton Olympus Fluoview FV1000-MPE microscope. CFP-expressing tumors were excited at a wavelength of 880nm using a 25X 1.05NA water objective with a 2.3x zoom. Time lapse imaging was done over 30 minutes, taking 2 minute intervals, collecting 5μm steps through a 100μm stack. Arrows indicate areas of cell motility. Scale bar = 25μm.

Additional File 4 Supplemental Figure 1. Immunohistochemistry indicates no difference in density of lymphatic vessels in the Neu primary tumors. Tumors from the Neu-NDL, Neu-YD, and Neu-YB were fixed in 10% buffered formalin, sectioned and stained using the LYVE-1 antibody against mouse Lymphatic Vessel Endothelial Receptor 1 to stain lymphatic endothelial cells. Representative images are shown from each strain, scale bar = 100μm.

Additional File 5 Supplemental Figure 2. The Neu-YB tumors show increased vasculature. Tumors from the Neu-NDL, Neu-YD, and Neu-YB strains were fixed in 10% buffered formalin, sectioned and stained using an endomucin antibody to detect vasculature. **(A.)** Quantification of vessels was done using a 20x objective. 10 random fields were counted per tumor, N= 3 tumors per strain. Data are means and SEM, * p <

0.05, ** $p < 0.005$, *** $p < 0.0005$. **(B.)** Representative images are shown for each strain, Scale bar = 100μm.

Additional File 6 Supplemental Figure 3. Further characterization of CXCL12 and CXCR4 in the Neu tumors. (**A.)** Primary culture cell lines were counted and seeded in duplicate and supernatants were collected for CXCL12 quantification 16 hours after cultures were confluent. ELISA was done in triplicate for each sample using the CXCL12 mouse ELISA from R&D systems. Data are means and SEM. **(B.)** Tumors from the Neu-NDL, Neu-YD, and Neu-YB strains were fixed in 10% buffered formalin, sectioned and stained using anti-CXCR4 antibody. Representative images are shown for each strain, Scale bar = 50μm **(C.)** mRNA was extracted from the Neu primary tumor cells in culture. Levels of CXCR4 are represented as average delta CT's normalized to Neu-NDL. N=3 samples per strain. Data are means and SEM. **(D.)** CXCL12-induced chemotaxis of primary tumor cells (top) or MTLn3 CXCR4 overexpressing cells (bottom) was determined using a microchemotaxis Boyden chamber assay. Data are means and SEM. **(E.)** *In vitro* wound healing assay with MTLn3 CXCR4 cells in the absence (Buffer) or presence of 1 nM CXCL12. Data are means and SEM, N = 3, 10 fields per condition. *P<0.05

Additional File 7 Supplemental Figure 4. MTLn3 GFP CXCL12 cell line overexpresses CXCL12 compared to empty vector control cells. MTLn3 GFP CXCL12 and MTLn3 GFP pQCXIP control lines were plated in triplicate and supernatants were collected from confluent cultures after 16 hours. Cells were counted to normalize for cell

number and an ELISA was done in triplicate for each sample using the CXCL12 mouse ELISA from R&D systems. Data are means and SEM, *** $p < 0.0005$.

Additional File 8 Supplemental Figure 5. Macrophage CXCR4 expression and responses to CXCL12. **(A**.) Expression of CXCR4 on tumor cells and macrophages in vivo. MTLn3 GFP CXCL12 and pQCXIP empty vector control primary tumors were dissociated, and labeled with CD45-AF700, F4/80-PerCP, and CXCR4-PE antibodies. Cells were washed and stained with DAPI as a viability marker. Samples were analyzed with flow cytometry and data was processed using FlowJo. Tumor cells were CD45-, F4/80-, GFP +. Macrophages were CD45+ and F4/80+. The mean fluorescence of CXCR4-PE is shown in representative images. N = 3 tumors for each cell line. **(B**.) Expression of CXCR4 on macrophages in vitro. Representative images of live murine bone marrow-derived macrophages (BMMs) stained for control or CXCR4 (*right panels*). Matched phase contrast images are shown (*left panels).* Scale bar = 10 μm. **(C.)** Chemotaxis of macrophages in vitro. CXCL12-induced chemotaxis of bone marrow-derived macrophages (BMMs) with 50 ng/ml CXCL12 was determined using a Transwell assay and expressed as cells per field. N = 3, mean ± S.E. ***, $p < 0.0003$.

Additional File 9 Supplemental Figure 6. Tumor volumes, lung metastasis and vasculature of MTLn3 GFP CXCL12 tumors. (**A.)** Tumor volumes were calculated by measuring the length and width of the tumor. There was no significant difference in tumor volume between the CXCL12 overexpressors and empty vector control. **(B.)** Lung

metastasis was quantified as total number of micrometastases in all lobes by H&E per section. The MTLn3 CXCL12 tumors displayed a trend for increased metastases. Error bars = SEM, N=10 mice. **(C.)** MTLn3 empty vector control and MTLn3 CXCL12 tumors were fixed in 10% buffered formalin, sectioned and stained using the endomucin antibody against the mouse endothelial cells to stain vasculature. Quantification of vessels was done using a 20x objective. 10 random fields were counted per tumor, N= 3 tumors per strain. Data are means and SEM, *** $p < 0.0002$. **(D. &E.)** Representative images are shown for the control (D) and CXCL12 (E) tumors, Scale bar = 100μm.

A.

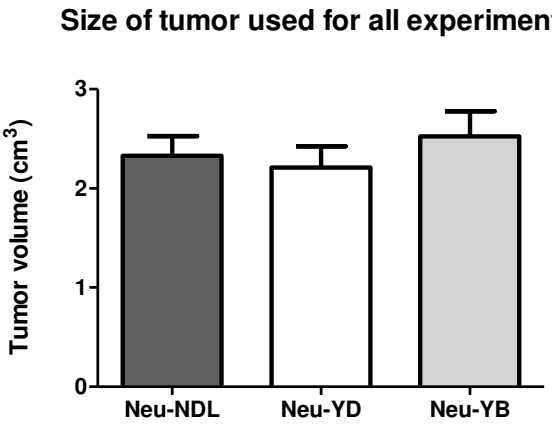
Size of tumor used for all experiments
Tumor volume (cm3)
3
2
1
0
Neu-NDL
Neu-YD
Neu-YB

B.

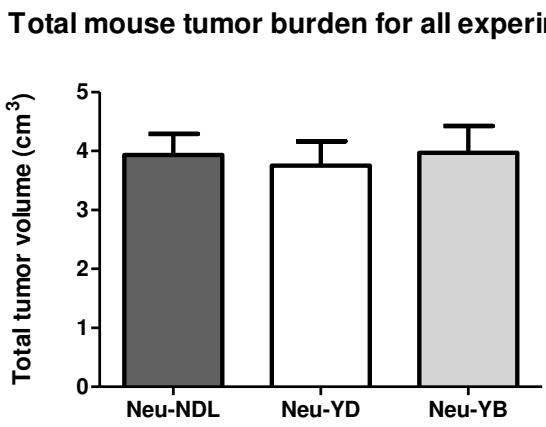
Total mouse tumor burden for all experiments
Total tumor volume (cm3)
5
4
3
2
1
0
Neu-NDL
Neu-YD
Neu-YB

C.

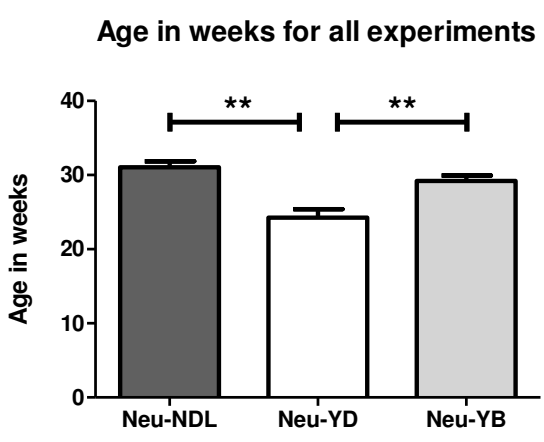
Age in weeks for all experiments
Age in weeks
40
30
20
10
0
**
**
Neu-NDL
Neu-YD
Neu-YB

Figure 1

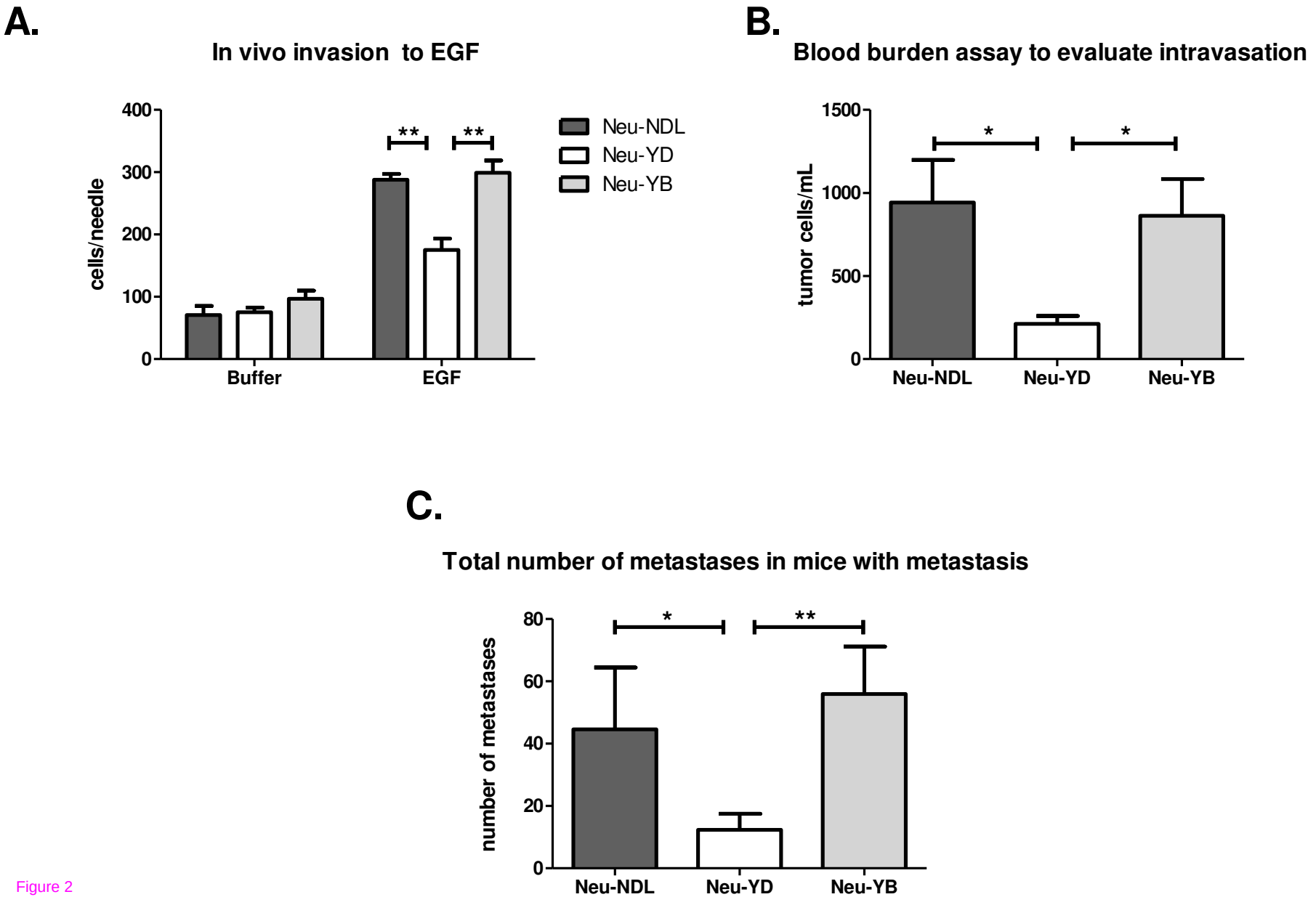
A.
In vivo invasion to EGF
cells/needle
400
300
200
100
0
**
**
Buffer
EGF
Neu-NDL
Neu-YD
Neu-YB
B.
Blood burden assay to evaluate intravasation
tumor cells/mL
1500
1000
500
0
*
*
Neu-NDL
Neu-YD
Neu-YB
C.
Total number of metastases in mice with metastasis
number of metastases
80
60
40
20
0
*
**
Neu-NDL
Neu-YD
Neu-YB

Figure 2

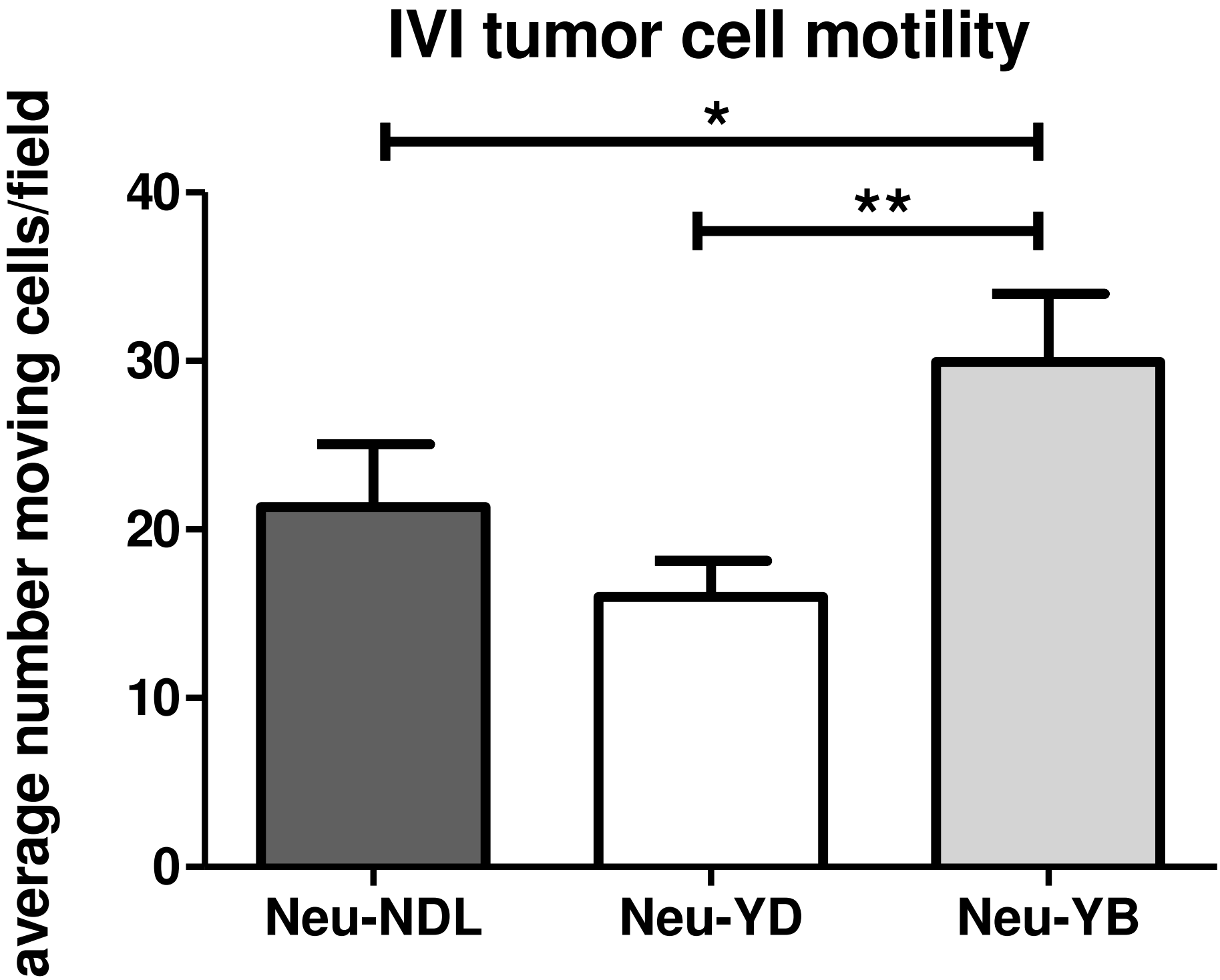
IVI tumor cell motility
average number moving cells/field
*
**
40
30
20
10
0
Neu-NDL
Neu-YD
Neu-YB

Figure 3

A.

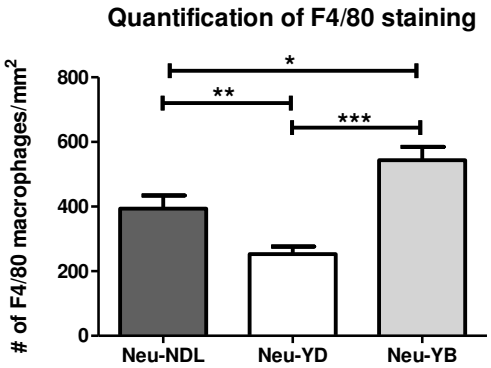
Quantification of F4/80 staining
# of F4/80 macrophages/mm2
800
600
400
200
0
*
**
***
Neu-NDL
Neu-YD
Neu-YB

B.

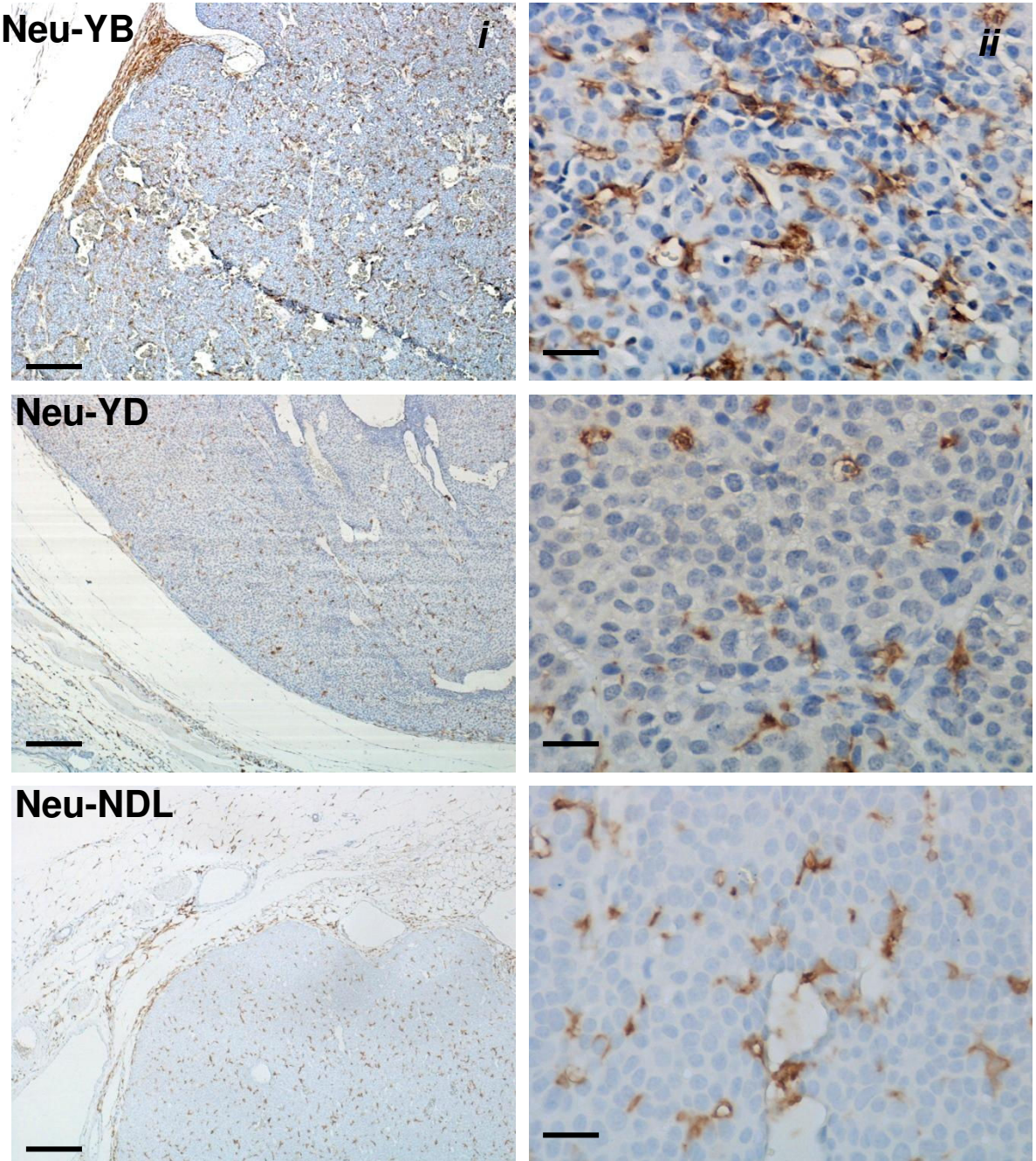
Neu-YB
i
ii
Neu-YD
Neu-NDL

Figure 4

A.

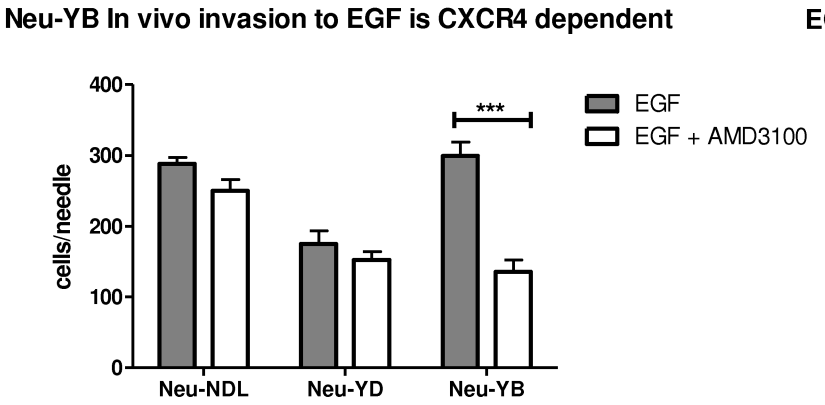

B.

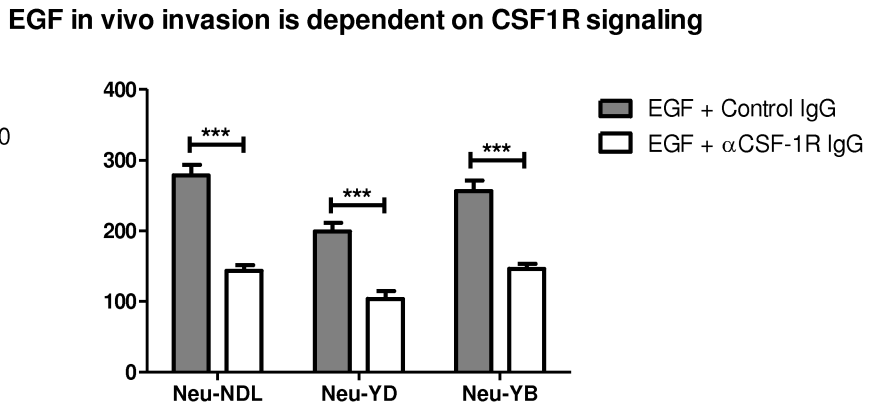

C.

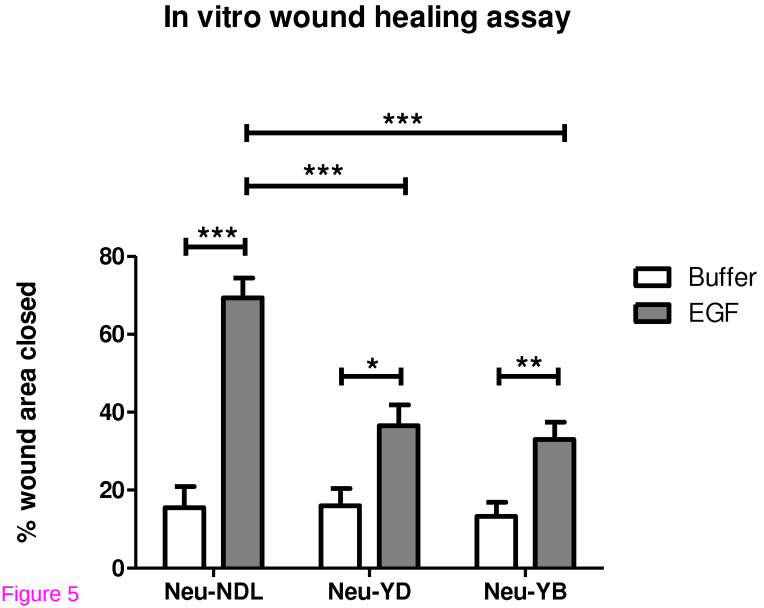

D.

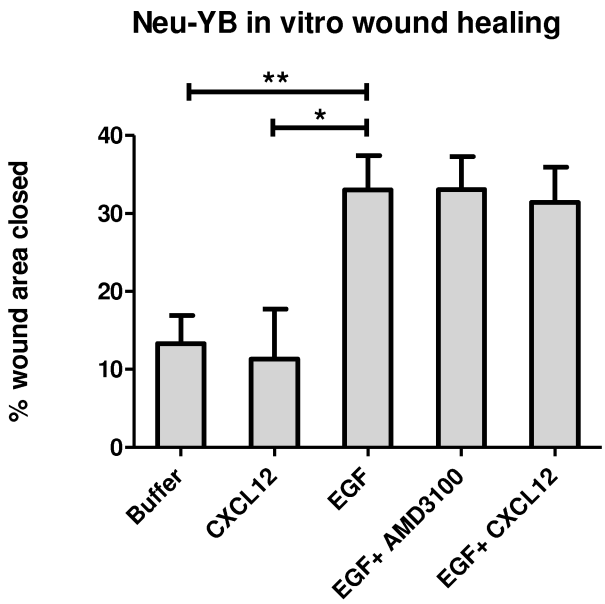

Figure 5

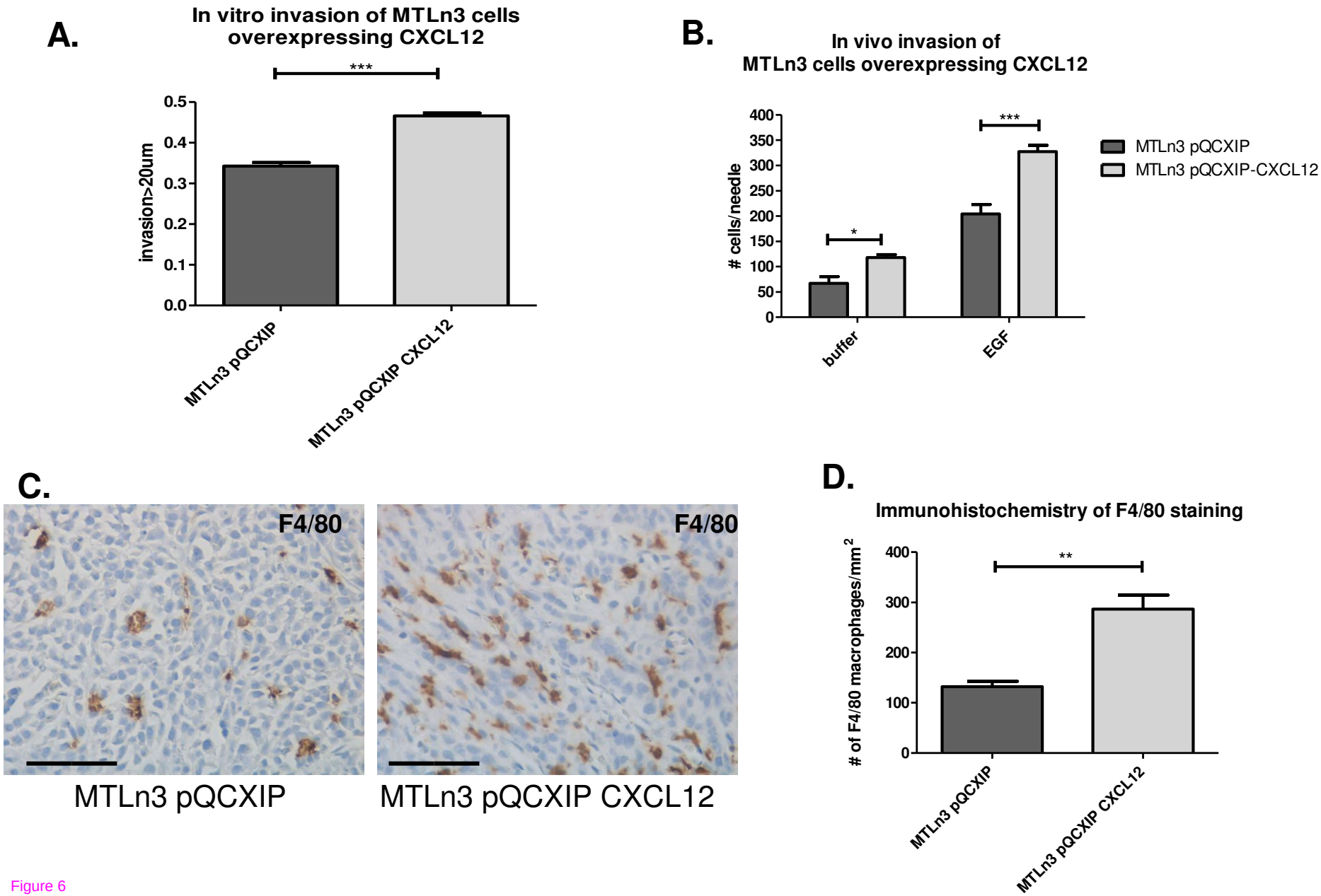
A.
In vitro invasion of MTLn3 cells overexpressing CXCL12
***
invasion>20um
0.5
0.4
0.3
0.2
0.1
0.0
MTLn3 pQCXIP
MTLn3 pQCXIP CXCL12
B.
In vivo invasion of MTLn3 cells overexpressing CXCL12
cells/needle
400
350
300
250
200
150
100
50
0
*
***
buffer
EGF
MTLn3 pQCXIP
MTLn3 pQCXIP-CXCL12
C.
F4/80
F4/80
MTLn3 pQCXIP
MTLn3 pQCXIP CXCL12
D.
Immunohistochemistry of F4/80 staining
# of F4/80 macrophages/mm2
400
300
200
100
0
**
MTLn3 pQCXIP
MTLn3 pQCXIP CXCL12

Figure 6

Additional files provided with this submission:

Additional file 1: Additional file 1 NDL.avi, 385K
http://breast-cancer-research.com/imedia/2075324949671677/supp1.avi
Additional file 2: Additional File 2 YD.avi, 499K
http://breast-cancer-research.com/imedia/4901680316716784/supp2.avi
Additional file 3: Additional File 3 YB.avi, 319K
http://breast-cancer-research.com/imedia/7695424696716795/supp3.avi
Additional file 4: Additional File 4 Supp Fig 1.ppt, 313K
http://breast-cancer-research.com/imedia/1440995912671678/supp4.ppt
Additional file 5: Additional File 5 Supp Fig 2.ppt, 378K
http://breast-cancer-research.com/imedia/7692536556716788/supp5.ppt
Additional file 6: Additional File 6 Supp Fig 3.ppt, 350K
http://breast-cancer-research.com/imedia/1148627386671678/supp6.ppt
Additional file 7: Additional File 7 Supp Fig 4.ppt, 114K
http://breast-cancer-research.com/imedia/1725155936671679/supp7.ppt
Additional file 8: Additional File 8 Supp Fig 5.ppt, 1433K
http://breast-cancer-research.com/imedia/1337747161671680/supp8.ppt
Additional file 9: Additional File 9 Supp Fig 6.ppt, 307K
http://breast-cancer-research.com/imedia/4870703206716806/supp9.ppt